agriculture

MDPI

*Article*

# Effects of Different Biomass Types on Pellet Qualities and Processing Energy Consumption

**Yantao Yang [1,2], Lei Song [1,2], Yuanna Li [1,2], Yilin Shen [1,2], Mei Yang [1,2], Yunbo Wang [1,2], Hesheng Zheng [3], Wei Qi [4] and Tingzhou Lei [1,2,*]**

[1] Institute of Urban and Rural Mining, Changzhou University, Changzhou 213164, China; yyt@cczu.edu.cn (Y.Y.); s22020817013@smail.cczu.edu.cn (L.S.)
[2] Changzhou Key Laboratory of Biomass Green, Safe & High Value Utilization Technology, Changzhou 213164, China
[3] M.I.P Technology (Changzhou) Co., Ltd., Changzhou 213164, China
[4] Guangdong Provincial Key Laboratory of New and Renewable Energy Research and Development, Guangzhou 510640, China
* Correspondence: leitingzhou@cczu.edu.cn

**Abstract:** This work conducts a single-factor experiment to study the effects of biomass types on the relax density, volume expansion, durability, hydrophobicity, and processing energy consumption. We analyze the differences in the quality of the pellets, and optimize the compaction conditions suitable for different biomass types including straw, hardwood, shell, and herbaceous plant. The results indicated that with a compressing force of 60~1500 N, compressing time of 10 s, powder size of less than 0.5 mm, and moisture content of 10%, the relax densities of corn straw, rice straw, selenium-rich rice straw, weigela japonica branches, and camphor leaves range from 360 to 820 kg/m$^3$, with a processing energy consumption of 17,360 to 28,740 J/kg; meanwhile, the relax densities of argy wormwood, forage grass, green grass, and peanut shells range from 340 to 840 kg/m$^3$, with a processing energy consumption of 33,510 to 73,700 J/kg. Therefore, the compaction pretreatment effectively regulates the density of biomass pellets and reduces the processing energy consumption. This study analyzed the differences in the quality of pellets caused by the inherent characteristics of biomass, providing strong support for the directional depolymerization and enhanced pretreatment technology for the scaled production of biomass alcohol fuels.

**Keywords:** biomass type; physicochemical property; compaction; pellet quality; processing energy consumption

Academic Editors: Janusz Gołaszewski

Received: 31 December 2024
Revised: 29 January 2025
Accepted: 29 January 2025
Published: 31 January 2025

**Citation:** Yang, Y.; Song, L.; Li, Y.; Shen, Y.; Yang, M.; Wang, Y.; Zheng, H.; Qi, W.; Lei, T. Effects of Different Biomass Types on Pellet Qualities and Processing Energy Consumption. *Agriculture* **2025**, *15*, 316. https://doi.org/10.3390/agriculture15030316



## 1. Introduction

In recent decades, due to urbanization and industrialization [1,2], the excessive use of traditional energy sources has led the world to face a significant energy crisis [3,4], impacting the environment and human health [5,6]. However, due to technological advancements and population growth, the demand for energy continues to rise [7], further exacerbating the current energy situation. Renewable energy sources, such as hydropower, wind energy, and bioenergy, can partially replace fossil fuels and alleviate the crisis. By 2018, renewable resources accounted for approximately 20% of global energy consumption, with biomass energy making up 9% of the total primary energy supply worldwide [8]. Particularly in some Nordic countries, biomass is commonly compressed

into pellets for use. In 2015, the global production of biomass pellets reached 25.6 million tons, and in 2016, global biomass pellet trade totaled 16.5 million tons [9]. China has abundant biomass resources, including crop straw, agricultural processing residues, forest residues, energy crops, municipal waste, and organic waste, amounting to approximately 460 million tons of standard coal equivalent each year [10]. Although over 700 million tons of straw are produced annually, they are dispersed over 100 million square kilometers of land [11,12], resulting in high transportation and processing costs, as well as difficulties in collection, storage, and transport [13,14]. Additionally, due to spatial and seasonal reasons, the supply is unstable [15], and the loose structure of biomass feedstocks is not suitable for long-term storage, limiting their large-scale processing and application [16].

Biomass compaction technology can convert amorphous and low-density feedstocks into "green", clean, and efficient fuel pellets under mechanical pressure [11,17,18], thereby improving the efficiency of biomass storage and transportation. According to different process characteristics, compaction technology is roughly divided into heating compaction, room temperature compaction, constant temperature and humidity compaction, and carbonization compaction [11]. The physical properties of the pellets mainly include bulk density and hydrophobicity, while the mechanical properties mainly include compressive strength and durability. Energy consumption is used as a production characteristic evaluation index [19], and these characteristics are mainly affected by various factors such as feedstock type, moisture content (4–15%), powder size (less than 2.5 mm), compaction pressure (60–130 MPa), heating temperature (343–423 K), and compaction method [20]. There are significant differences in the physical and mechanical properties of different biomass pellets, which have a considerable impact on their storage, transportation, and utilization. An appropriate pressure is conducive to forming a dense and compact structure, helping pellets maintain their integrity and stability. Stelte et al. [21] found that as the pressure increases, the pellet density significantly increases, and when the pressure exceeds 250 MPa, the density slightly increases. Moreover, the compaction pressure is influenced by various factors such as the biomass type, moisture content, particle size, and temperature. The moisture contained in the feedstocks can act as a natural lubricant [22]. Additionally, an excessively low moisture content can reduce the ductility and increase the friction between pellets, leading to increased energy consumption; whereas an excessively high moisture content can reduce the compactness between particle layers [23], making compaction difficult. Therefore, the moisture content needs to be controlled based on an assumed ideal state, precisely regulating the ratio of dry feedstocks to moisture and adjusting the compaction process parameters. Under higher humidity conditions, due to the compact structure and higher bulk density of the pellets, the hydrophobicity is enhanced to a certain extent, allowing them to resist moisture absorption from the air, reducing water permeability, and thereby enhancing the pellets' ability to withstand storage environments [24,25]. Pellets encountering open flames during transportation may cause explosions [26,27], posing safety issues. To minimize transportation costs and reduce the fire risk caused by dust explosions [28], pellets must not suffer physical damage during compaction and use.

Conventional biomass densification is aimed at producing fuel pellets with high energy density, with a density controlled between 1100 and 1400 kg/m$^3$. This study addresses transportation issues caused by the variability of different biomass types, thus using compaction technology to product lower density (500–700 kg/m$^3$) pellets from crushed feedstocks, saving space and requiring lower energy consumption , which is beneficial for improving the transportation efficiency and reducing production costs. The impact of different pellets on the physical and mechanical properties was explored, with selected biomass categories including straw, wood, shells, and herbs. First, the chemical composition and physicochemical properties of the feedstocks were determined and analyzed. Then, the amount of feedstock added was precisely controlled to adjust the density

of the pellets and analyze their volume expansion changes. Finally, by combining morphological characteristics and hydrophobicity, the physical quality was evaluated, and the relationship between energy consumption and relaxed density was established. The compressor used is of the constant stroke control type, so under the same compression displacement conditions, the volume of the pellets remains consistent. In industrial pelletizing practice, appropriate molds need to be designed based on the technical parameters of the compressor, and the maximum capacity of the mold used is about 5 $cm^3$, requiring prior vibration of the feedstocks before compaction. The final pellets produced need to be transported to alcohol fuel processing plants for crushing treatment. The stability of compacted pellets is relatively low, with a high breakage rate and low energy requirements, followed by an acid-base pretreatment to improve quality, and, finally, high-quality biomass ethanol is produced through enzymatic fermentation and other technical means. Therefore, the significance of this research lies in utilizing compaction technology to provide lower density pellets, addressing the long-distance transportation and storage issues of different biomass feedstocks, and combining compaction parameters and production energy consumption to comprehensively assess the application value of different biomass pellets, enhancing their market competitiveness, thereby meeting the needs for the diversity and differentiation of storage, utilization, and efficient transportation.

## 2. Materials and Methods

### *2.1. Experimental Materials and Equipment*

Biomass feedstocks exhibit significant differences in their compaction characteristics. According to categories, the experimental feedstocks included straw (corn straw (CS), rice straw (RS), and selenium-rich rice straw (SS)), hardwood (weigela japonica branches (WJ) and camphor leaves (CLs)), shell (peanut shells (PSs)), and herbaceous plant (argy wormwood (AW), forage grass (FG), and green grass (GR)), as shown in Figure 1. A grinding machine (CM100M, Glitterman Instrument Equipment Co., Ltd., Beijing, China) was used to crush the feedstocks, and powder smaller than 0.5 mm was screened and sealed for subsequent compaction experiments.

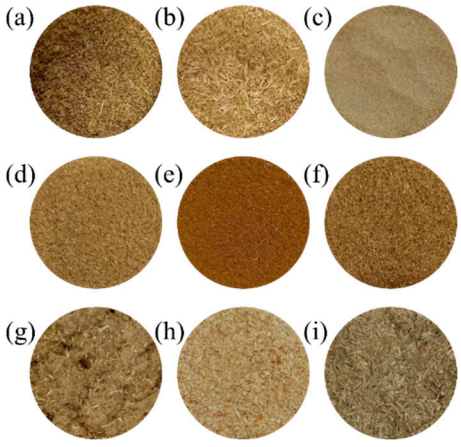


**Figure 1.** Topography diagram of corn straw (**a**), rice straw (**b**), selenium-rich rice straw (**c**), weigela japonica branches (**d**), camphor leaves (**e**), peanut shells (**f**), argy wormwood (**g**), forage grass (**h**) and green grass (**i**).

An automatic hydraulic press (Y32-5T, Lituo Machinery Co., Ltd., Zhengzhou, China) was used to compact the pellets; its parameters are shown in Table 1. The four-column hydraulic press with vertical structure has an independent power mechanism and electrical system, adopts button centralized control (YJ32-50T cartridge valve integrated

system), and is equipped with a jog and semi-automatic working system (with automatic return function). The hydraulic power system is composed of energy conversion devices (pump and cylinder), energy regulating devices (valves), and energy transmission devices (oil tank and pipeline). With the control of the electrical system, the movable beam is driven to move, and the fixed-range compaction process action cycle is completed by adjusting the working pressure, pressing speed, and stroke. The fuselage is connected by the upper beam, the movable beam and the lower beam are connected by four columns, and a closed rigid frame is formed by tightening the nut to withstand the hydraulic press. When working, the movable beam and the piston rod of the main cylinder are connected, and the column is oriented to move up and down. The stroke limit device is composed of a guide plate and a stroke switch, and adjusts different stroke switch positions for the upper limit stroke switch.

**Table 1.** Technical parameters of the hydraulic press.

| The Name of Parameters | Value | Unit |
|---|---|---|
| Compressing force | 50,000 | N |
| Maximum stroke of movable beam | 250 | mm |
| Maximum opening height | 300 | mm |
| Height of the workbench from the ground | 750 | mm |
| Workbench length | 300 | mm |
| Workbench width | 200 | mm |
| The diameter of pellet | 8 | mm |
| The length of pellet | 12 | mm |
| Empty up speed | 2~3 | mm/s |
| Work speed | 1~2 | mm/s |
| Return speed | 4 | mm/s |
| Total power of the device | 1500 | W |

The compaction process mainly includes the hydraulic press, compressing mold, force sensor (JHBM-4, Zhongwan Jinnuo Sensor Co., Ltd., Bengbu, China), intelligent display control instrument (MCK-Z-I), and data acquisition module (Modbus communication mode, capable of real-time dynamic display of load values, number of acquisition points, and experimental curves), as shown in Figure 2. The hydraulic press can operate under various load forces monitored by a force sensor (80,000 N, accuracy 0.01 N), allowing precise control and maintenance of test force, deformation, and displacement.

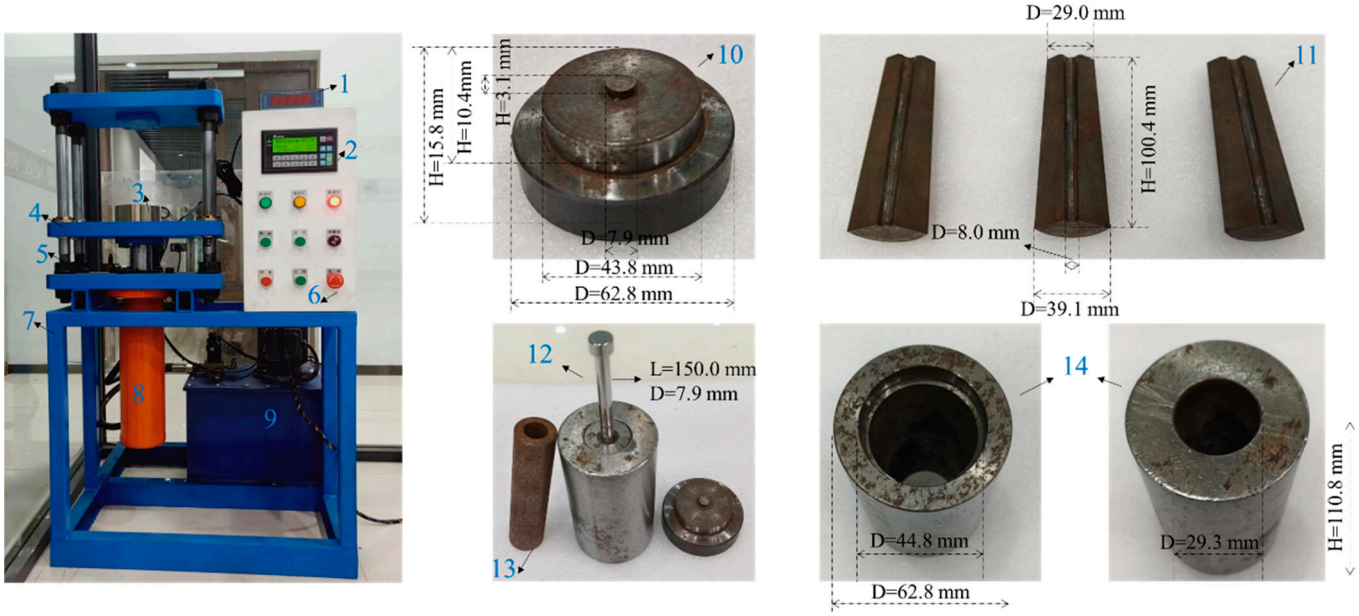


**Figure 2.** Structure diagram of hydraulic press and compaction module. ((1) Intelligent display control instrument, (2) guide plate, (3) force sensor, (4) workbench, (5) movable beam, (6) stroke switch,

(7) fuselage, (8) cylinder, (9) oil tank, (10) mold base, (11) inner mold, (12) thimble, (13) mold opener, (14) mold sleeve).

### 2.2. Compressing Methods

The working principle of the hydraulic press is to determine the compressing force by controlling the displacement, changing the mass to ensure that the biomass feedstocks can be compressed into pellets, and then judging the durability, finally optimizing the compaction conditions to precisely regulate the pellet density. The compaction process of biomass feedstocks is shown in Figure 3.

(1) The biomass feedstocks should be added to the compressing mold; then, gently tap it.
(2) Place the compressing mold on the workbench, adjust the vertical alignment of the thimble with the mold, keeping the end of the thimble at the same level as the top of the mold, and then set the parameters to the automatic compressing.
(3) The compression should be carried out at a speed of 2.0 mm/s. Stop when the set displacement value should be reached, and maintain it for 10 s (to inhibit the rebound effect); then, the compressing force should be recorded.
(4) Use the mold opener to demold, and gently tap the inner mold to ensure the integrity of the pellets with small cylinders.
(5) An analytical balance with an accuracy of ±0.001 g should be used to measure the mass of pellets, and the electronic caliper with an accuracy of ±0.01 mm should be used to measure the diameter and length. Finally, the processing energy consumption is evaluated.

Repeat the above steps (1)~(5) to make at least 3 granules of each feedstock. During compression, the mass of the pellet does not change. Other operating parameters are as follows: the biomass feedstock is pre-dried, 10% water should be added using a pipette according to the mass ratio (9:1), stirred, covered with cling film, and left for 12 h until the moisture is evenly mixed, no binder should be added. At room temperature (298 ± 5 K), the compacted pellets are 8 mm in diameter and 12 mm in length. The dependent variable is the amount of feedstock added (0.360, 0.420, 0.480, 0.540, 0.600, and 0.660 g) and the corresponding independent variable is the compressing force.

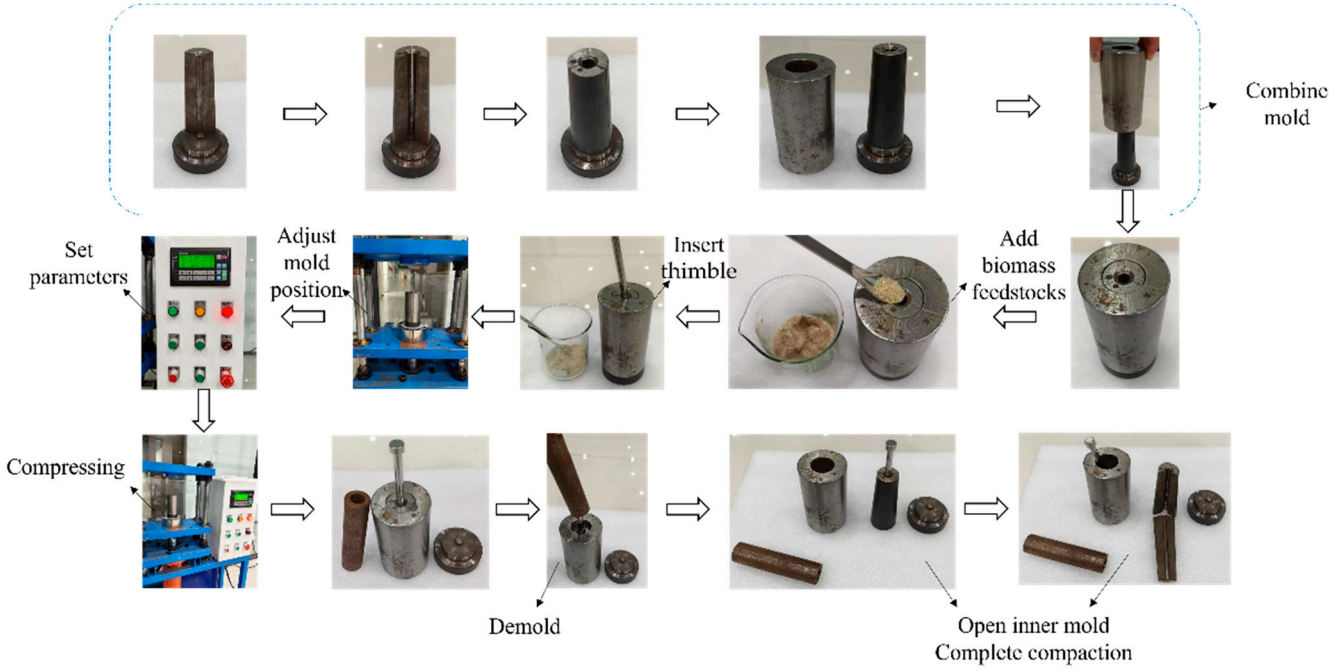


**Figure 3.** Schematic diagram of the compaction process of biomass feedstocks.

### *2.3. Determination of Physicochemical Properties of Biomass Feedstocks*

#### 2.3.1. Determination of Proximate Analysis

According to the "Proximate analysis Method for Solid Biomass Fuels (GB/T 28731-2012)" [29], the ash and volatile of biomass feedstocks were determined using a box furnace (KF1200, Boyuntong Instrument Technology Co., Ltd., Nanjing, China).

#### 2.3.2. Determination of Ultimate Analysis

The C, H, N, and S element contents were measured using an organic elemental analyzer (Vario MACRO Cube, Germany Elementar).

#### 2.3.3. Determination of Calorific Value

Based on [30], the higher calorific value was determined using an oxygen bomb calorimeter (HYHW-8A, Huayu Instrument Co., Ltd., Hebi, China).

#### 2.3.4. Determination of Bulk Density and Tap Density

We used a natural bulk density meter (FBS-1003, Forbes Testing Equipment Co., Ltd., Xiamen, China) to measure the bulk density. We placed the dried biomass powder inside the funnel, opened the piston, and allowed them to flow into the graduated cylinder (50 mL). We used a ruler to level the powder surface along the edge of the cylinder, and calculated the bulk density using Equation (1).

$$\rho_{(bd/td)} = \frac{m_T - m_{gc}}{V_{gc}} \quad (1)$$

where $\rho_{bd}$ is the bulk density, kg/m$^3$; $\rho_{td}$ is the tap density, kg/m$^3$; $m_{gc}$ is the mass of the graduated cylinder, kg; $m_T$ is the total mass of the graduated cylinder and the powder, kg; and $V_{gc}$ is the volume of the graduated cylinder, m$^3$. (The volume of compaction of pellets is about $6 \times 10^{-5}$ m$^3$.)

According to the "Powders–Determination of tap density (GB/T 21354-2008)" [31], we held a graduated cylinder by hand and gently tapped it on a thick rubber pad to prevent the surface of the powder from loosening until the powder volume was no longer reduced. If the surface was uneven, we read the average value of the highest and lowest points of the surface after tapping as the tap volume. The calculation method for the tap density was the same as the bulk density in Equation (1).

### *2.4. Evaluation Indicators and Measurement Methods for Biomass Pellets*

The physical properties of biomass pellets include density, chemical composition, calorific value, moisture content, ash content, volatile content, fixed carbon content, etc. The mechanical properties include shape and size, breakage rate, slag formation, combustion characteristics, durability and stability, and the processing energy consumption during the compaction process.

#### 2.4.1. Determination of Compaction Density

Biomass compaction process mainly includes two parts: compressing and demolding [32]. The density of the pellets is the compaction density ($\rho_{cd}$) after demolding and the relax density ($\rho_{rd}$) measured after 120 min, calculated using Equation (2) [33].

$$\rho_{cd} = \frac{4m_c}{\pi d^2 h} \quad (2)$$

where $\rho_{cd}$ is the compaction density of the pellets, kg/m$^3$; $m_c$ is the mass, kg; $d$ is the diameter, m; and $h$ is the height, m.

2.4.2. Determination of Volume Expansion

The volume expansion refers to the ratio of the volume of biomass pellets after compaction and expansion to the volume when not expanded. Biomass pellets with a higher volume expansion will create more voids during the combustion process, which helps with the diffusion of oxygen and improves combustion efficiency. However, the ash produced during combustion may affect the operational efficiency and lifespan of combustion equipment. Therefore, understanding the volume expansion of biomass pellets is beneficial for improving combustion efficiency and the characteristics of combustion products, as well as reducing particulate emissions. We calculated the volume expansion based on the data of $\rho_{cd}$ and $\rho_{rd}$, as in Equation (3).

$$V_E = \frac{V_r}{V_c} = \frac{m_r/\rho_{rd}}{m_c/\rho_{cd}} = \frac{\rho_{cd}}{\rho_{rd}} \quad (3)$$

where $V_E$ is the volume expansion of the pellets; $\rho_{cd}$ is the compaction density, kg/m$^3$; and $\rho_{rd}$ is the relax density, kg/m$^3$. During the compaction process, the mass changes less; hence, $m_r$ is approximately equal to $m_c$.

2.4.3. Determination of Durability

We placed the pellets on a vibrating screen at a speed of 120 rpm for 10 min, and measured durability by calculating the remaining mass percentage of the pellets after mechanical vibration [34], as in Equation (4).

$$D = \frac{m_w}{m_c} \times 100 \quad (4)$$

where $D$ is the durability index, %; $m_c$ is the mass of the pellets, kg; and $m_w$ is the mass after mechanical vibration, kg.

2.4.4. Determination of Hydrophobicity

We placed the pellets in a constant temperature and humidity chamber (HWS-50, Shangcheng Instrument Manufacturing Co., Ltd., Shaoxing, China) at a temperature of 303 K and humidity of 70%, measuring the mass of the pellets every 30 min until the weight change remained stable after continuous weighing, indicating that the pellets have reached a saturated moisture equilibrium state, and recorded the moisture content at this time as the equilibrium moisture content, calculated as in Equation (5) [35].

$$EMC = \frac{(m_e - m_c)}{m_c} \times 100 \quad (5)$$

where $EMC$ is the equilibrium moisture content of the pellets, %; $m_c$ is the mass, kg; and $m_e$ is the mass when the water absorption reaches equilibrium, kg.

2.4.5. Determination of Processing Energy Consumption

The energy required for biomass compaction mainly depends on the compressing force and moisture content, and is also related to the physical properties of the biomass feedstocks and the compressing method. Although the compaction work is independent of the size of the pressing channel, the demolding process requires more energy due to friction and the smaller cross-sectional area of the pressing channel [32]. The compressing mold designed in this experiment had side seams on the inner side of the sleeve, allowing easy sampling by gently tapping the top of the mold, which reduced the energy needed for demolding. The work required for compressing the biomass feedstocks was determined through force-displacement values, calculated as in Equation (6) [36].

$$W = \sum_{i=1}^{n} F_i \times S_i \quad (6)$$

where $F_i$ is the compressing force at time i, N; and $S_i$ is the displacement at time i, m.

The compressing force can be collected through the intelligent display instrument at the force sensor signal conversion end, while the displacement value was calculated as in Equation (7).

$$S = \frac{4M}{\pi d^2 \rho_{td}} \quad (7)$$

where $M$ is the mass of the biomass powder, kg; $d$ is the diameter of the pellets, m; and $\rho_{td}$ is the tap density, kg/m$^3$.

Processing energy consumption is the energy consumed per unit mass of the powder during the compaction process, calculated as in Equation (8).

$$w = \frac{W}{m_c} = \frac{\sum_{i=1}^{n} F_i \times S_i}{m_c} = \frac{\int_1^n FdS}{m_c} \quad (8)$$

where $w$ is the processing energy consumption, J/kg; $W$ is the total work, J; $m_c$ is the mass of the pellets, kg; $F$ is the compressing force, N; $S$ is the compressing displacement, m; i is the instantaneous compressing displacement value; and n is the end compressing displacement value.

## 3. Results and Discussion

### *3.1. Physicochemical Properties of Biomass Feedstocks*

Table 2 presents the proximate and ultimate analysis of different biomass feedstocks. The ash content of RS and SS was relatively high, at 12.55% and 12.81%; the fixed carbon content of CS and WJ was relatively high, at 13.72% and 13.83%; the volatile content of CLs and FG was relatively high, at 89.77% and 90.09%. The ultimate analysis shows that the carbon content of CLs and PSs was relatively high, at 54.98% and 51.77%; their oxygen content was relatively low, at 36.61% and 32.06%. The hydrogen content of different biomass feedstocks was similar, while the nitrogen and sulfur contents were low, which is beneficial for subsequent energy and resource utilization.

**Table 2.** Proximate analysis, ultimate analysis, and density of corn straw, rice straw, selenium-rich rice straw, weigela japonica branches, camphor leaves, peanut shells, argy wormwood, forage grass, and green grass.

| Biomass Feedstocks | Proximate analysis (%, Dry Basis) | | | Ultimate Analysis (%, Dry Ash-Free Basis) | | | | | HHV (×10$^6$ J/kg) | Bulk Density (kg/m$^3$) | Tap Density (kg/m$^3$) |
|---|---|---|---|---|---|---|---|---|---|---|---|
| | Ash | Fixed Carbon | Volatile | C | H | O* | N | S | | | |
| CS | 4.84 ± 0.05 | 13.72 ± 0.14 | 81.44 ± 0.81 | 39.17 ± 0.39 | 5.78 ± 0.06 | 54.25 ± 0.54 | 0.74 ± 0.01 | 0.06 ± 0.00 | 18.64 ± 0.56 | 150 ± 1.50 | 260 ± 2.60 |
| RS | 12.55 ± 0.13 | 11.93 ± 0.12 | 75.52 ± 0.76 | 48.08 ± 0.48 | 6.57 ± 0.07 | 44.13 ± 0.44 | 0.99 ± 0.01 | 0.23 ± 0.00 | 19.82 ± 0.59 | 180 ± 1.80 | 260 ± 2.60 |
| SS | 12.81 ± 0.13 | 7.59 ± 0.08 | 79.60 ± 0.80 | 47.51 ± 0.48 | 6.80 ± 0.07 | 44.65 ± 0.45 | 0.78 ± 0.01 | 0.26 ± 0.00 | 19.86 ± 0.60 | 220 ± 2.20 | 360 ± 3.60 |
| WJ | 3.83 ± 0.04 | 13.83 ± 0.14 | 82.34 ± 0.82 | 50.34 ± 0.50 | 6.90 ± 0.07 | 40.30 ± 0.40 | 1.94 ± 0.02 | 0.52 ± 0.01 | 21.39 ± 0.64 | 330 ± 3.30 | 490 ± 4.90 |
| CL | 8.50 ± 0.09 | 1.73 ± 0.02 | 89.77 ± 0.90 | 54.98 ± 0.55 | 7.17 ± 0.07 | 36.61 ± 0.37 | 1.08 ± 0.01 | 0.16 ± 0.00 | 23.64 ± 0.71 | 320 ± 3.20 | 420 ± 4.20 |
| PS | 6.63 ± 0.07 | 9.75 ± 0.10 | 83.62 ± 0.84 | 51.77 ± 0.52 | 6.43 ± 0.06 | 39.24 ± 0.39 | 2.41 ± 0.02 | 0.15 ± 0.00 | 20.74 ± 0.62 | 230 ± 2.30 | 340 ± 3.40 |
| AW | 7.71 ± 0.08 | 4.40 ± 0.04 | 87.89 ± 0.88 | 50.46 ± 0.50 | 6.98 ± 0.07 | 40.96 ± 0.41 | 1.41 ± 0.01 | 0.19 ± 0.00 | 20.74 ± 0.62 | 150 ± 1.50 | 200 ± 2.00 |
| FG | 3.16 ± 0.03 | 6.75 ± 0.07 | 90.09 ± 0.90 | 50.12 ± 0.50 | 6.77 ± 0.07 | 42.68 ± 0.43 | 0.34 ± 0.00 | 0.09 ± 0.00 | 20.23 ± 0.61 | 180 ± 1.80 | 250 ± 2.50 |
| GR | 7.62 ± 0.08 | 4.44 ± 0.04 | 87.94 ± 0.88 | 44.52 ± 0.45 | 6.46 ± 0.06 | 47.43 ± 0.47 | 1.31 ± 0.01 | 0.28 ± 0.00 | 17.18 ± 0.52 | 180 ± 1.80 | 280 ± 2.80 |

O*: calculated by difference.

From Table 2, it can be seen that after the biomass powder is tapped under natural accumulation conditions, the bulk density and tap density vary because physical

structures are determined by different chemical component contents. The mass of CS, RS, and SS per unit volume increased by 110 kg, 80 kg, and 140 kg; the mass of WJ, CLs, and PSs increased by 160 kg, 100 kg, and 110 kg; the mass of AW, FG, and GR increased by 50 kg, 70 kg, and 100 kg. AW had the lowest bulk density (150 kg/m$^3$) compared to FG and GR, indicating that it is relatively loose, with the largest gaps between powder particles. In the same volume, the mass proportion from largest to smallest was WJ, CLs, PSs, SS, GR, FG, RS, CS, and AW. It can be seen that the powder density of wood was larger, with smaller gaps between powder particles, resulting in a harder structural composition, consuming more energy; meanwhile, the powder density of straw and herbaceous was smaller, with lower bulk density in a natural state, occupying more space for the same mass of feedstocks, resulting in a loose structural composition requiring lower compressing force and consuming less energy. Eisenbies et al. [37] studied three bulk density measurement methods that provided different results for commercial-scale harvesting of willow biomass chips. Bulk density is an important value for decision making that has implications throughout the supply chain, so it is important to have values based on measurements from equipment that would be used for commercial-scale operations. Based on this study, single values for the bulk density obtained from the literature should be used with some caution and understanding that values for a feedstock like straw and wood may be quite variable depending on a number of factors such as the collection equipment, crop characteristics, and field conditions.

### *3.2. Physical Properties of Biomass Pellets*

Figure 4 shows the compaction characteristics of biomass feedstocks. As the compressing force increases, the compaction density increases and the volume expansion decreases. An appropriately high compressing force can destroy the microstructure of biomass feedstocks, form a new phase structure, and increase the strength and stiffness of the product, resulting in the biomass pellets becoming more compact and reducing the volume. Higher densities generally result in a better durability, reflecting the ability of a pellet to resist breakage when subjected to external forces. Therefore, there is a mutual relationship between the compressing force (Figure 4a), compaction density (Figure 4b), volume expansion (Figure 4c), and durability (Figure 4d). A proper compressing force can increase the density of pellets, reduce the volume expansion, and improve the durability. From Figure 4c,f, the relax density of CS pellets is 440~820 kg/m$^3$, which is prone to plastic rebound, with a volume expansion of 1.32~1.39. CS has larger diameter vessels, allowing moisture to be transmitted smoothly and providing lubrication; due to the high cellulose content in CS, the powder can effectively bond during plastic deformation, enhancing the bonding strength between particles. The relax density of RS pellets is 360~640 kg/m$^3$, with a volume expansion of 1.70~2.00. RS consists of inner and outer glumes connected by two hook-like structures, and, due to the high silica content, it is covered by a layer of siliceous feedstock, making it a hard short-fiber straw. During the compaction process, it is prone to breakage due to the compressing force, resulting in a relatively uniform small powder. Under equal deformation displacement, the compressing force on RS is 60~500 N, which is relatively high and can be attributed to its high ash content, leading to insufficient compressing space for the small powder after compaction and fragmentation. Its rich silica characteristics prevent moisture within the powder from adequately transferring and bonding, failing to effectively reduce friction. As the compressing force increases, the relax density of SS is 400~710 kg/m$^3$, with a volume expansion of 1.50~1.74. As the gaps between powder particles decrease, the compaction density gradually increases, and when the density reaches a certain level, it stabilizes, with the height of the pellets remaining basically unchanged, mainly because its density approaches that of the particle cell walls [38].

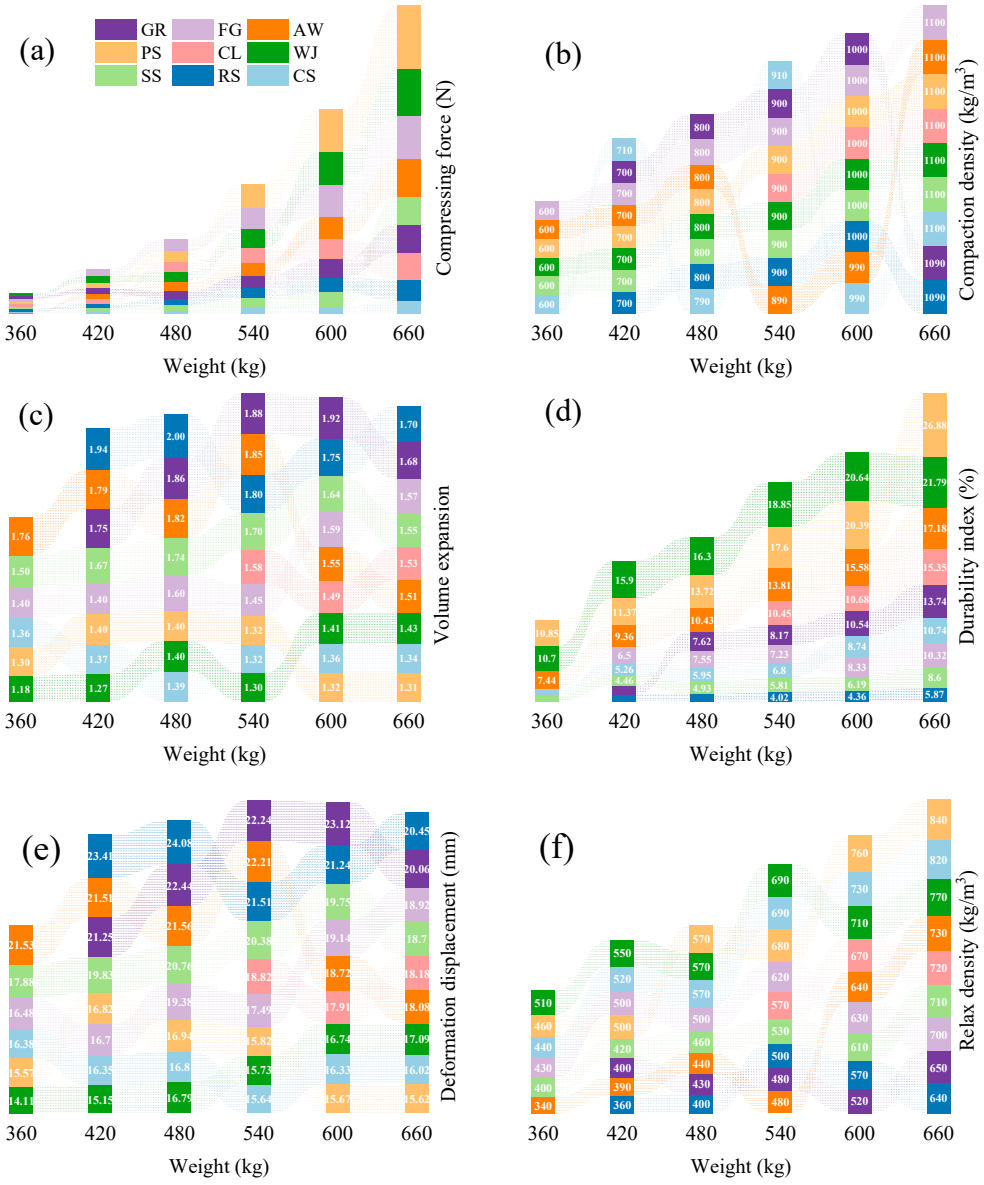


**Figure 4.** Compaction characteristics of corn straw (CS), rice straw (RS), selenium-rich rice straw (SS), weigela japonica branches (WJ), camphor leaves (CLs), peanut shells (PSs), argy wormwood (AW), forage grass (FG), and green grass (GR). As the weight of the feedstocks increases, the changes in compressing force (**a**), compaction density (**b**), volume expansion (**c**), durability index (**d**), deformation displacement (**e**), and relax density (**f**).

From Figure 4c,f, it can be seen that the relax density of WJ pellets is 510~770 kg/m$^3$, with minimal plastic rebound and tight bonding, and a volume expansion of 1.18~1.43. The relax density of CL pellets is 570~720 kg/m$^3$, with a volume expansion of 1.49~1.58, showing minimal expansion and lower bonding properties. The relax density of PSs is 460~840 kg/m$^3$, which is relatively high; the volume expansion is 1.30~1.40. PSs have a high content of lignin and epidermal fibers, and, after crushing, they produce many mesh-like feedstocks. During the compaction process, due to the high degree of lignification in PSs, their long and tough fibers require more energy to break the mesh into small powder, resulting in the maximum compressing force needed during the same deformation displacement being 60~1500 N.

From Figure 4c,f, it can be seen that the relax densities of AW, FG, and GR pellets are 340~730 kg/m$^3$, 430~700 kg/m$^3$, and 400~650 kg/m$^3$, with significant plastic rebound; the volume expansion is 1.51~1.85, 1.40~1.60, and 1.68~1.92, showing high expansion. The fats

and waxes contained in herbs reduce the interaction between particles during the compaction process, lowering the compressing forces between adjacent particles and causing a decrease in their bonding strength, leading to expansion phenomena. Due to the differences in the inherent characteristics of different biomasses, as well as the changes in internal moisture and shear stress of the pellets, the compaction density gradually decreases after demolding, while the volume expansion continuously increases and tends to stabilize with prolonged placement time. During the compaction process, in the radial direction, herb particles bond and fully extend through interlocking [39], while in the axial direction, herb particles contact each other and bond through van der Waals forces, electrostatic forces, and adsorption layers, with axial expansion being much greater than radial expansion [40]. Therefore, there are significant differences in the relax densities and volume expansion of CS, RS, SS, WJ, CLs, PSs, AW, FG, and GR, and the compaction quality is influenced by various factors. The compaction characteristics of different biomasses show obvious differences, attributed to their varying structural compositions and component content, along with uneven powder sizes, leading to significant variations in the difficulty of compaction.

From Figure 4e, it can be seen that when the biomass feedstocks amount is 480 kg and the compressing force is 150 N, the deformation displacement of RS is the largest, at 24.08 mm; when the biomass feedstocks amount is 360 kg and the compressing force is 70 N, the deformation displacement of WJ is the smallest, at 14.11 mm; when the biomass feedstocks amount is 660 kg, the deformation displacement of AW, FG, and GR is 18.08, 18.92, and 20.06 mm, indicating a relatively large deformation displacement, attributed to the relatively large vascular bundles of the herbaceous plants, which are easily crushed and undergo plastic deformation. As the compressing force increases, the gaps between the herbaceous powder are mostly filled, plastic deformation becomes dominant, and the shape and position of the pellets change, accompanied by a rupture and reordering during deformation. When the compressing force is 300 ± 50 N, the deformation sizes of different biomasses are in the order of GR > AW > RS > SS > FG > CLs > PSs > WJ > CS. The factors affecting the durability are quite complex, arising not only from the chemical composition and structure of the biomass itself, but also being related to moisture content, compressing force, and compressing time among other external factors. Due to the mutual effect between the biomass powder particles and between the powder and equipment, along with the corresponding shear stress, the pellets are prone to breakage and powder loss. At the same biomass feedstocks amount, the pellets of CS, WJ, PSs, and AW exhibit good durability, making them less likely to scatter during transportation, thus enhancing their physical quality.

The pellet density is an important physical property closely related to storage requirements and energy density [41]. All compaction densities and relax densities vary with different types of feedstocks. The relax density of all pellets slightly decreased, especially for herbaceous pellets, due to the most pronounced rebound effect. A higher compaction density indicates a higher pellet quality, while a higher relax density indicates greater potential and suitability for compaction. Comparing the compaction density and relax density of pellets with the bulk density of feedstocks, the density of straw feedstocks increased by 1.1 to 3.2 times through the compaction process, wood feedstocks increased by 1.0 to 1.7 times, herbaceous feedstocks increased by 1.4 to 3.7 times, and PSs increased by 1.3 to 2.5 times. The volume expansion is a comparison of the changes in density, since pellets dry and rebound during storage. Pellets with a smaller absolute value of the expansion ratio have greater stability [42]. Volume expansion occurs at points where the length of the pellets is greater than their diameter, as the applied force is primarily in the radial direction. The expansion ratio is a positive value, with the main changes being length and diameter expansion, demonstrating that biomasses are elastic feedstocks. Straw and herbaceous feedstocks exhibit more expansion, while wood feedstocks and PSs

have lower expansion. Under the parameters of the compaction process, pellets mainly exhibit a slight plastic deformation. The pellet strength is an indicator of hardness and durability, and is directly related to the pellet density and the applied force [41,42]. Higher durability is suitable for transportation and storage, with minimal production of fine powder. Lower durability may lead to pores and gaps, reducing the resistance to deformation [43].

Figure 5 shows the apparent physical morphology of biomass pellets. As shown, under the compaction conditions of 298 ± 5 K, compressing force of 60~1500 N, compressing time of 10 s, powder size less than 0.5 mm, and moisture content of 10%, the surfaces of biomass pellets exhibit different physical morphologies. The pellets of CS (Figure 5a) show no obvious cracks and have a good compaction effect, indicating strong bonding between the particles. The pellets of RS (Figure 5b) and SS (Figure 5c) have relatively smooth surfaces with very few gaps, indicating good bonding effects between the powder; however, a layered cross-section is also observed, further confirming the "layering" phenomenon [44], where there are many fillers between the layers, which act as solid bridges to ensure bonding. Therefore, the compaction pellets have a poor shear resistance, leading to decreased durability. The pellets of CLs (Figure 5e) are soft and easily loosen, with weak bonding between powder particles and a poor compaction effect. The pellets of WJ (Figure 5d) and PSs (Figure 5f) have smooth and flat surfaces, with no obvious plastic rebound, and almost no visible gaps between powder particles. The long fibers in the cross-section are intertwined, mechanical interlocking and a network structure, which can effectively resist the fracture force caused by plastic rebound after compressing, resulting in significant bonding strength. Additionally, fillers can be observed between the powder particles, mainly due to lignin being extruded from the cells to the particle surface under a high compressing force, softening through frictional heating, and crystallizing between particles upon cooling, creating solid bridges that effectively enhance the bonding strength between particles. Since WJ and PSs contain a higher lignin content, the number of solid bridges is greater, leading to better relax density, and thus greater durability. The pellets of AW (Figure 5g), FG (Figure 5h), and GR (Figure 5i) have uneven surfaces with many gaps, which is a major factor for their low relax density, also indicating less contact area between powder particles, resulting in better durability. The outer surfaces of AW, FG, and GR powders are covered with a thick cuticle, and the wax in the cuticle hinders hydrogen bonding between particles, leading to a reduced bonding strength; the presence of the waxy layer reduces the van der Waals forces between the waxy layer and the particles, and the thicker waxy layer exacerbates its cohesive failure.

Considering the physical properties of biomass feedstocks, the structure and design of molds, and the compaction process, some biomass pellets exhibit inherent defects [45]. Cracked pellets are a common defect that typically occurs during storage due to moisture loss and feedstock rebound, as shown in Figure 5. Ignoring the negative effect on pellet strength and hardness, fractured pellets may have better combustion performance. Broken pellets mean fewer solid bridges and weaker short-range forces (hydrogen bonding, van der Waals forces, and electrostatic forces) [46]. The chemical composition of feedstocks varies, and the essence of converting feedstocks into pellets is the comprehensive effect of heat, moisture, compressing force, friction, and mechanical shear on hemicellulose, cellulose, lignin, starch, proteins, fats, and oils during the compaction process [46]. The distribution of feedstocks in the mold channel and the forces applied during compaction can affect the rebound of the feedstock and cause bending, attributed to the entanglement and folding of hemicellulose, cellulose, and lignin between the pellets and fibers [46]. Bending pellets are also considered a result of the elasticity and plasticity of different biomass feedstocks. The combination of suitable compaction equipment molds, a reasonable compaction process, and high-quality biomass feedstocks is essential to avoid these defects in the pellets [47].

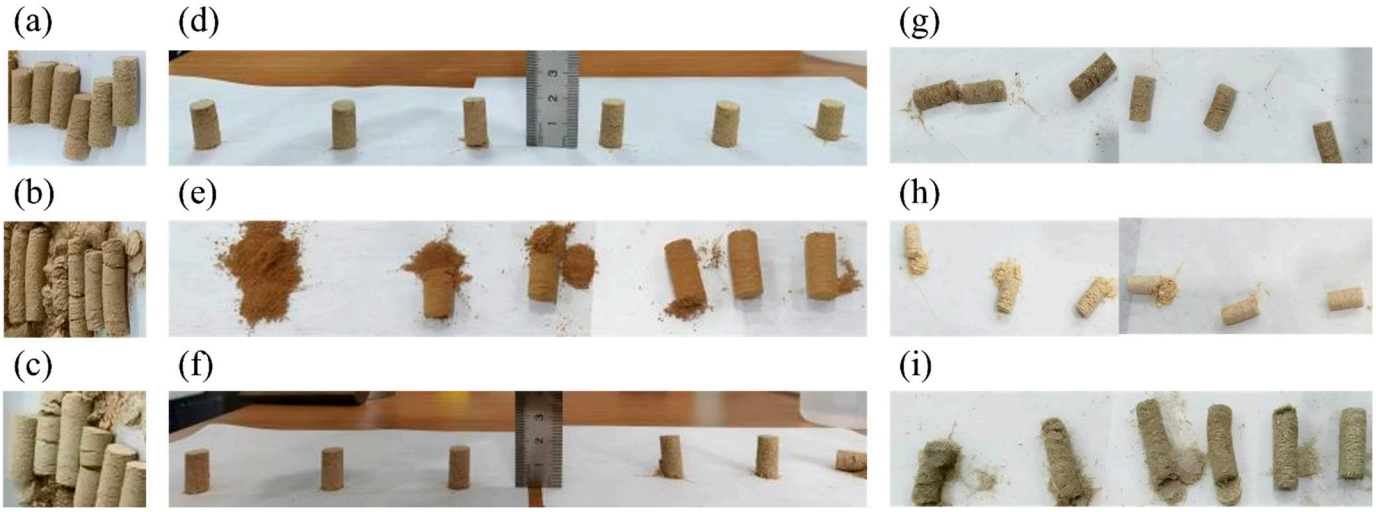


**Figure 5.** Compaction pellets of corn straw (**a**), rice straw (**b**), selenium-rich rice straw (**c**), weigela japonica branches (**d**), camphor leaves (**e**), peanut shells (**f**), argy wormwood (**g**), forage grass (**h**), and green grass (**i**). The pellet volume was consistent, the compressing force gradually increased, and the mass was 0.360, 0.420, 0.480, 0.540, 0.600, and 0.660 g.

Figure 6 shows the water absorption characteristic curve of biomass pellets at a humidity of 70%. As shown, the water absorption rate of CS (Figure 6a) and SS (Figure 6c) pellets is relatively fast. When the water absorption time reaches 2400 min, the absorption rate slows down, and after 7200 min, the maximum water absorption content is 4.24% and 2.45%, which is beneficial for enhancing the transfer and bonding between particles. The dehydration rate of RS (Figure 6b) is relatively slow: when the dehydration time reaches 120 min, the water absorption content approaches saturation, with a maximum dehydration amount of 0.18%. This is because although RS contains a higher amount of polar substances [48], the long fibers entangle under a higher compressing force, greatly increasing the interaction and bonding forces between particles [49], effectively improving the relax density and reducing the surface porosity, ensuring good hydrophobicity. The maximum dehydration amount of WJ (Figure 6d) pellets is 0.98%, indicating high hydrophobicity due to their higher relax density, making the pellets relatively compact with fewer surface gaps, making it difficult for moisture to penetrate. The maximum dehydration amount of CL (Figure 6e) pellets is 1.60%, showing the best hydrophobicity; when the water absorption time is 120 min, the dehydration amount is 0.38%, and after 960 min, it approaches equilibrium and remains basically unchanged. This is attributed to the fact that CLs contain a significant amount of non-polar and stable silica inorganic compounds. During the compaction process, the crushed feedstocks have fewer pores, making it difficult for moisture to penetrate. The water absorption rate of PS (Figure 6f) pellets is relatively low; when the water absorption time is 1200 min, it approaches saturation with a water absorption content of 0.30%, and after 7200 min, the maximum moisture content is 0.48%. The maximum dehydration amounts of AW (Figure 6g), FG (Figure 6h), and GR (Figure 6i) pellets are 1.08%, 0.24%, and 0.62%, indicating high hydrophobicity, which is attributed to the lower relax density and loose structure of the herbaceous pellets, as well as their higher surface porosity and numerous fine-diameter vessels, making it difficult for moisture to penetrate.

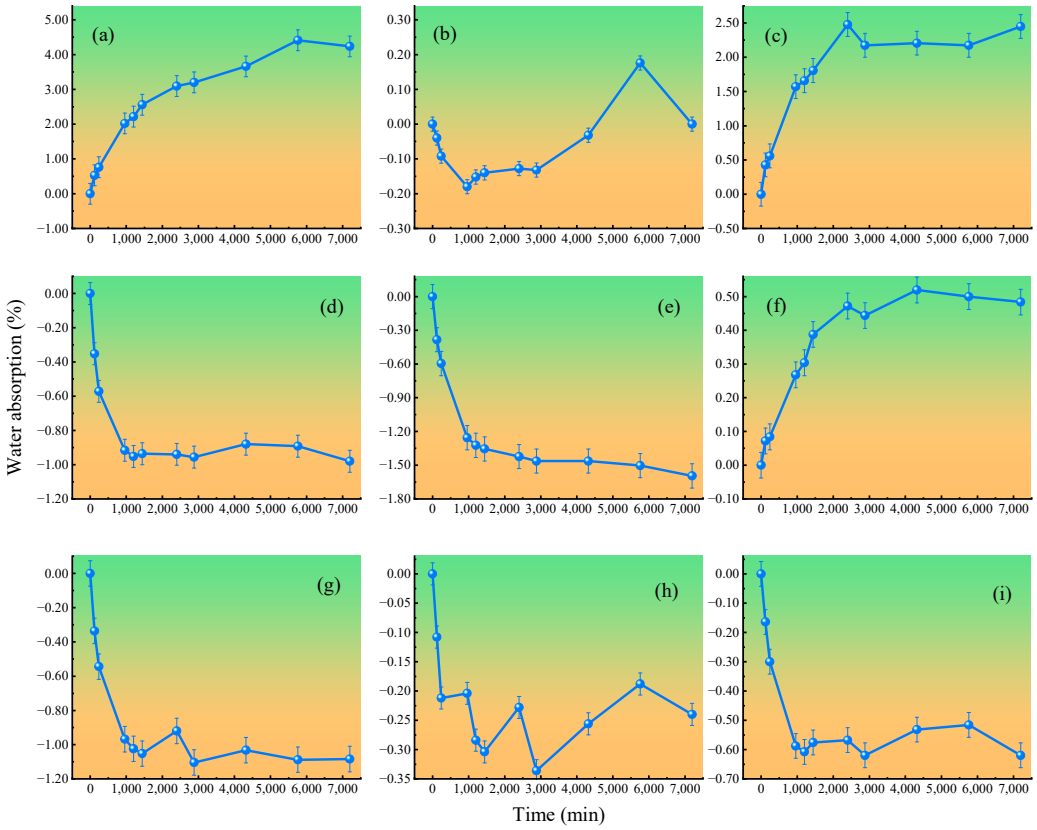


**Figure 6.** Hydrophobicity of corn straw (**a**), rice straw (**b**), selenium-rich rice straw (**c**), weigela japonica branches (**d**), camphor leaves (**e**), peanut shells (**f**), argy wormwood (**g**), forage grass (**h**), and green grass (**i**).

Due to the hydrophobicity of the biomass feedstocks, a different biomass has different compaction characteristics. The hydrophobicity of the compaction pellets is closely related to the type of feedstocks and the processing techniques used. Biomass feedstocks contain a certain amount of moisture, and during the compaction process, some of this moisture will be lost, thereby affecting the hydrophobicity. Compaction technology can increase the density of biomass feedstocks, thereby enhancing their hydrophobicity. The hydrophobicity also has an effect on the environment; higher hydrophobicity means that less smoke and harmful gases are produced during combustion, thus reducing environmental pollution. Therefore, improving the hydrophobicity of biomass feedstocks not only helps to enhance their combustion efficiency, but also contributes to reducing their environmental effect. Additionally, compacted and pre-treated biomass pellets, due to increased hydrophobicity, can reduce the moisture and energy required for fungal growth, thereby achieving the goal of inhibiting fungal proliferation [50], which is also significant for the long-term storage and transportation of biomass.

### *3.3. Processing Energy Consumption*

Figure 7 shows the processing energy consumption during the compaction process. As illustrated, there are significant differences in the processing energy consumption of different biomass pellets, and the influence of the biomass's own organizational structure on its compaction quality varies. The processing energy consumption of CS (Figure 7a) pellets is 17,360 J/kg. This is mainly because CS has a high cellulose content, and its epidermal fiber structure easily undergoes plastic deformation, requiring a lower compressing energy to ensure that the fiber structures in the powder can bond and intertwine with each other during rearrangement, as well as the solid bridges and hydrogen bonds between the particles inside the pellets. The processing energy consumption of RS (Figure

7b) pellets is 28,740 J/kg, with a tendency to exhibit delamination phenomena [44]. RS has thick cell walls, small lumen, and characteristics of rigid short fibers, making it prone to collapse. However, due to the high ash content, the powder surface is covered with a layer of silica and its inorganic compounds [51], presenting a three-dimensional network structure. The chemical properties of these silica compounds are very stable and have high hardness, making it difficult for adjacent particles to come into close contact and generate intermolecular forces. At the same time, silica and its inorganic compounds are non-polar substances, which also makes it difficult for particles to generate electrostatic adhesion, leading to a reduced relax density. The processing energy consumption of SS (Figure 7c) pellets is 24,750 J/kg, which is second only to that of RS. Since the chemical composition of SS is similar to that of RS, the plasticity of the silica and its inorganic compounds it contains is very poor. The pellets mainly rely on the stacking of particle sheets, using higher processing energy consumption to form solid bridges between the sheets and layer upon layer, resulting in strong shear stress in the radial direction and lower mechanical resistance in the axial direction.

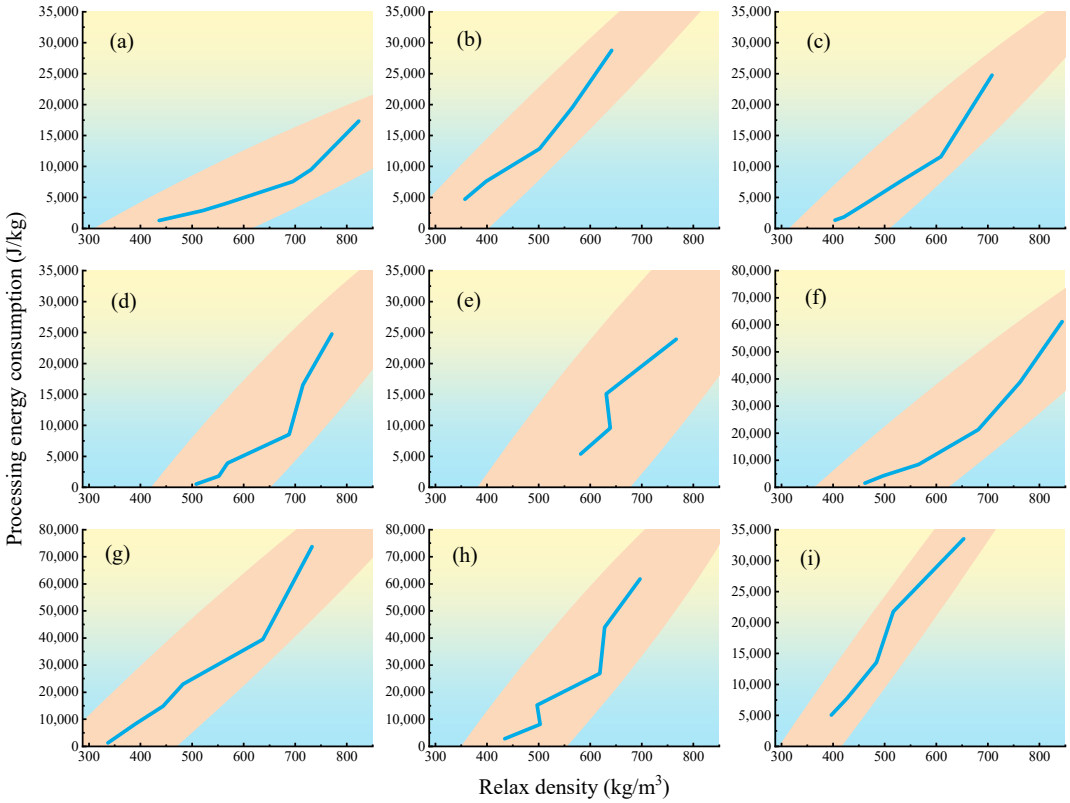


**Figure 7.** Processing energy consumption of corn straw (**a**), rice straw (**b**), selenium-rich rice straw (**c**), weigela japonica branches (**d**), camphor leaves (**e**), peanut shells (**f**), argy wormwood (**g**), forage grass (**h**), and green grass (**i**).

The processing energy consumption of WJ (Figure 7d) pellets is 24,750 J/kg, which is relatively high, mainly due to the high lignin content and degree of lignification of WJ. The epidermal fibers are longer and more resilient, requiring higher compressing energy to ensure that the powder can bond together and form a compact structure. The processing energy consumption of CL (Figure 7e) pellets is 18,630 J/kg, with smaller powder gaps and higher hydrophobicity, exhibiting low plastic deformation under a lower compressing force, and the original compact structure has not undergone rearrangement. The processing energy consumption of PS (Figure 7f) pellets is the highest at 61,160 J/kg, due

to their hard texture and stable structural composition, requiring more energy to disrupt the intermolecular forces between particles, thereby enhancing the bonding strength.

The processing energy consumption of AW (Figure 7g) pellets is 73,700 J/kg, with a relax density slightly higher than that of FG and GR, while the processing energy consumption of FG (Figure 7h) pellets is 61,780 J/kg, and that of GR (Figure 7i) pellets is 33,510 J/kg, all of which have lower processing energy consumption than AW pellets. During the compaction process, fats and waxes in FG and GR are pressed to the surface of the pellets, providing some lubrication, which reduces the friction between the powder particles and between the powder and the mold, resulting in a lower processing energy consumption. Herbaceous crops contain a high content of extracts, primarily consisting of fats and waxes, so the powder surfaces are covered with a layer of polyester keratin derived from fatty acids. The keratin layer reduces the interactions between particles, preventing the formation of solid bridges and hydrogen bonds, limiting the van der Waals forces and mechanical interlocking between particles [49], ultimately leading to a decrease in their bonding strength.

The processing energy consumption largely depends on the types of biomass feedstock. The herbaceous feedstocks and PS were the highest, followed by straw and woody feedstocks. Herbaceous feedstocks with a lower cellulose content and lignin content had a greater processing energy consumption, with AW having the highest processing energy consumption, approximately 10 times that of the lowest, CS (700 kg/m$^3$). Proteins or fats can be extruded from plant cells and form an oil film on the pellet surface, acting as lubricants and reducing the friction between the pellet surface and the mold inner wall. Evaluating processing energy consumption from the perspective of chemical composition, fats are the best, followed by starch, proteins, pectin, and cell walls (hemicellulose, cellulose, and lignin) [46].

## 4. Conclusions

A comprehensive evaluation from biomass feedstocks to pellets was investigated to explore the potential of emerging different biomass feedstocks for compaction. The physical properties of biomass feedstocks were measured and evaluated.

Under the compaction conditions of the biomass feedstock with an amount of 360~660 kg, a compressing force of 60~1500 N, a compressing time of 10 s, a powder size of less than 0.5 mm, and a moisture content of 10%, there were differences in the physical quality of pellets. As the compressing force increases, the pellet density increases, the volume expansion decreases, it becomes more compact, and the durability increases. The relax densities of pellets from CS, RS, and SS were 440~820 kg/m$^3$, 360~640 kg/m$^3$, and 400~710 kg/m$^3$; the volume expansion was 1.32~1.39, 1.70~2.00, and 1.50~1.74. The relax densities of pellets from WJ and CL were 510~770 kg/m$^3$ and 570~720 kg/m$^3$, while the volume expansion was 1.18~1.43 and 1.49~1.58. The relax density and volume expansion of PS pellets were 460~840 kg/m$^3$ and 1.30~1.40. The relax densities of AW, GR, and FG were 340~730 kg/m$^3$, 400~650 kg/m$^3$, and 430~700 kg/m$^3$; the volume expansion was 1.51~1.85, 1.68~1.92, and 1.40~1.60. After compression, the structure of the biomass changed, making it denser and more compact, which is beneficial for large-scale storage and transportation, saving stacking space. Therefore, understanding the volume expansion of biomass pellets is of great significance for optimizing the compaction process, and the density can be better regulated.

Under the compaction conditions of the biomass feedstock with an amount of 660 kg, there were differences in the processing energy consumption among different pellets. The processing energy consumption of pellets from CS, RS, and SS was 17,360 J/kg, 28,740 J/kg, and 24,750 J/kg. The processing energy consumption of pellets from WJ and CLs was 24,750 J/kg and 18,630 J/kg. The processing energy consumption of PS pellets was 61,160

J/kg. The processing energy consumption of AW, GR, and FG was 73,700 J/kg, 33,510 J/kg, and 61,780 J/kg. The type of biomass has a significant effect on the processing energy consumption. Although different biomasses can be compressed under the same compaction conditions, the physical properties of the pellets vary significantly with the differences in the biomass's structural composition and chemical components.

Further research will focus on improving the poor performance of feedstocks and pellets, as well as optimizing the compaction process. This work demonstrates that an analysis of the type of differentiation for emerging biomass feedstocks before compaction can instruct industrial production and predict pellet qualities.

**Author Contributions:** Project administration, funding acquisition, supervision, writing—review and editing, Y.Y.; conceptualization, data curation, writing—original draft, L.S.; investigation, validation, Y.L.; software, investigation, Y.S.; software, M.Y.; investigation, Y.W.; visualization, H.Z.; formal analysis, W.Q.; resources, project guidance, methodology, T.L. All authors have read and agreed to the published version of the manuscript.

**Funding:** This work was supported by the National Key Research and Development Program of China (No. 2022YFB4201901) and the Guangdong Provincial Key Laboratory of New and Renewable Energy Research and Development (No. E439kf0501).

**Institutional Review Board Statement:** Not applicable.

**Data Availability Statement:** The data used to support the findings of this study are available from the corresponding author upon request.

**Conflicts of Interest:** Author Hesheng Zheng was employed by the company M.I.P Technology (Changzhou). The remaining authors declare that the research was conducted in the absence of any commercial or financial relationships that could be construed as potential conflicts of interest.

## References

1. Hanif, M.U.; Capareda, S.C.; Kongkasawan, J.; Iqbal, H.; Arazo, R.O.; Baig, M.A. Effects of Pyrolysis Temperature on Product Yields and Energy Recovery from Co-Feeding of Cotton Gin Trash, Cow Manure, and Microalgae: A Simulation Study. *PLoS ONE* **2016**, *11*, e0152230. https://doi.org/10.1371/journal.pone.0156565.
2. Siloto, R.M.P.; Weselake, R.J. Site saturation mutagenesis: Methods and applications in protein engineering. *Biocatal. Agric. Biotechnol.* **2012**, *1*, 181–189. https://doi.org/10.1016/j.bcab.2012.03.010.
3. Nanda, S.; Berruti, F. Municipal solid waste management and landfilling technologies: A review. *Environ. Chem. Lett.* **2021**, *19*, 1433–1456. https://doi.org/10.1007/s10311-020-01100-y.
4. Nanda, S.; Berruti, F. Thermochemical conversion of plastic waste to fuels: A review. *Environ. Chem. Lett.* **2021**, *19*, 123–148. https://doi.org/10.1007/s10311-020-01094-7.
5. Ljung, K.; Schoon, P.L.; Rudolf, M.; Charrieau, L.M.; Ni, S.; Filipsson, H.L. Recent Increased Loading of Carbonaceous Pollution from Biomass Burning in the Baltic Sea br. *ACS Omega* **2022**, *7*, 35102–35108. https://doi.org/10.1021/acsomega.2c04009.
6. Fawzy, S.; Osman, A.I.; Doran, J.; Rooney, D.W. Strategies for mitigation of climate change: A review. *Environ. Chem. Lett.* **2020**, *18*, 2069–2094. https://doi.org/10.1007/s10311-020-01059-w.
7. Guo, J.; Li, C.-Z.; Wei, C. Decoupling economic and energy growth: Aspiration or reality? *Environ. Res. Lett.* **2021**, *16*, 044017. https://doi.org/10.1088/1748-9326/abe432.
8. Wei, Z.; Cheng, Z.; Shen, Y. Recent development in production of pellet fuels from biomass and polyethylene (PE) wastes. *Fuel* **2024**, *358*, 130222. https://doi.org/10.1016/j.fuel.2023.130222.
9. Haykiri-Acma, H.; Yaman, S. Effect of co-combustion on the burnout of lignite/biomass blends: A Turkish case study. *Waste Manag.* **2008**, *28*, 2077–2084. https://doi.org/10.1016/j.wasman.2007.08.028.
10. Zhang, X.; Gao, B.; Zhao, S.; Wu, P.; Han, L.; Liu, X. Optimization of a "coal-like" pelletization technique based on the sustainable biomass fuel of hydrothermal carbonization of wheat straw. *J. Clean. Prod.* **2020**, *242*, 118426. https://doi.org/10.1016/j.jclepro.2019.118426.

11. Zhou, Y.; Zhang, Z.; Zhang, Y.; Wang, Y.; Yu, Y.; Ji, F.; Ahmad, R.; Dong, R. A comprehensive review on densified solid biofuel industry in China. *Renew. Sustain. Energy Rev.* **2016**, *54*, 1412–1428. https://doi.org/10.1016/j.rser.2015.09.096.
12. Hong, H.; Ye, W.H.; Song, B.; Zhang, X.X. An empirical study on industrialization of biomass briquette in China. *Resour. Sci.* **2010**, *32*, 2172–2178. Available online: https://www.resci.cn/EN/Y2010/V32/I11/2172 (accessed on 5 October 2024).
13. Lestander, T.A.; Rudolfsson, M.; Pommer, L.; Nordin, A. NIR provides excellent predictions of properties of biocoal from torrefaction and pyrolysis of biomass. *Green Chem.* **2014**, *16*, 4906–4913. https://doi.org/10.1039/c3gc42479k.
14. Sokhansanj, S.; Fenton, J. Cost Benefit of Biomass Supply and Pre-Processing. 2006. Available online: https://www.cesarnet.ca/biocap-archive/rif/report/Sokhansanj_S.pdf (accessed on 10 November 2024).
15. Yue, D.; You, F.; Snyder, S.W. Biomass-to-bioenergy and biofuel supply chain optimization: Overview, key issues and challenges. *Comput. Chem. Eng.* **2014**, *66*, 36–56. https://doi.org/10.1016/j.compchemeng.2013.11.016.
16. Mousa, E.; Kazemi, M.; Larsson, M.; Karlsson, G.; Persson, E. Potential for Developing Biocarbon Briquettes for Foundry Industry. *Appl. Sci.* **2019**, *9*, 5288. https://doi.org/10.3390/app9245288.
17. Li, H.; Liu, X.; Legros, R.; Bi, X.T.; Jim Lim, C.; Sokhansanj, S. Pelletization of torrefied sawdust and properties of torrefied pellets. *Appl. Energy* **2012**, *93*, 680–685. https://doi.org/10.1016/j.apenergy.2012.01.002.
18. Chen, L.; Xing, L.; Han, L. Renewable energy from agro-residues in China: Solid biofuels and biomass briquetting technology. *Renew. Sustain. Energy Rev.* **2009**, *13*, 2689–2695. https://doi.org/10.1016/j.rser.2009.06.025.
19. Chen, T.; Jia, H.; Zhang, S.; Sun, X.; Song, Y.; Yuan, H. Optimization of Cold Pressing Process Parameters of Chopped Corn Straws for Fuel. *Energies* **2020**, *13*, 652. https://doi.org/10.3390/en13030652.
20. Mostafa, M.E.; Hu, S.; Wang, Y.; Su, S.; Hu, X.; Elsayed, S.A.; Xiang, J. The significance of pelletization operating conditions: An analysis of physical and mechanical characteristics as well as energy consumption of biomass pellets. *Renew. Sustain. Energy Rev.* **2019**, *105*, 332–348. https://doi.org/10.1016/j.rser.2019.01.053.
21. Stelte, W.; Holm, J.K.; Sanadi, A.R.; Barsberg, S.; Ahrenfeldt, J.; Henriksen, U.B. Fuel pellets from biomass: The importance of the pelletizing pressure and its dependency on the processing conditions. *Fuel* **2011**, *90*, 3285–3290. https://doi.org/10.1016/j.fuel.2011.05.011.
22. Hansted, A.L.S.; Nakashima, G.T.; Martins, M.P.; Yamamoto, H.; Yamaji, F.M. Comparative analyses of fast growing species in different moisture content for high quality solid fuel production. *Fuel* **2016**, *184*, 180–184. https://doi.org/10.1016/j.fuel.2016.06.071.
23. Fakhrabadi, E.A.; Kajzer, C.; Stickel, J.J.; Liberatore, M.W. Transport of Compressed Woody Biomass: Correlating Rheology and Microcompounder Measurements. *Ind. Eng. Chem. Res.* **2021**, *60*, 11470–11478. https://doi.org/10.1021/acs.iecr.1c00967.
24. Mundhada, S.; Chaudhry, M.M.A.; Erkinbaev, C.; Paliwal, J. Non-Destructive Quality Monitoring of Flaxseed During Storage. *J. Food Meas. Charact.* **2022**, *16*, 3640–3650. https://doi.org/10.1007/s11694-022-01464-5.
25. Saeed, A.A.H.; Yub Harun, N.; Bilad, M.R.; Afzal, M.T.; Parvez, A.M.; Roslan, F.A.S.; Abdul Rahim, S.; Vinayagam, V.D.; Afolabi, H.K. Moisture Content Impact on Properties of Briquette Produced from Rice Husk Waste. *Sustainability* **2021**, *13*, 3069. https://doi.org/10.3390/su13063069.
26. Liu, L.; Wang, D.; Gao, L.; Duan, R. Distributed heating/centralized monitoring mode of biomass briquette fuel in Chinese northern rural areas. *Renew. Energy* **2020**, *147*, 1221–1230. https://doi.org/10.1016/j.renene.2019.09.086.
27. Thek, G.; Obernberger, I. (Eds.) *The Pellet Handbook: The Production and Thermal Utilisation of Biomass Pellets*; Hardback: Carrum Downs, Victoria, 2011; p. 549, ISBN: 978-1-84407-631-4. https://doi.org/10.4324/9781849775328.
28. Hedlund, F.H.; Astad, J.; Nichols, J. Inherent hazards, poor reporting and limited learning in the solid biomass energy sector: A case study of a wheel loader igniting wood dust, leading to fatal explosion at wood pellet manufacturer. *Biomass Bioenergy* **2014**, *66*, 450–459. https://doi.org/10.1016/j.biombioe.2014.03.039.
29. *GB/T 28731-2012[S]*; General Administration of Quality Supervision, Inspection and Quarantine of the People's Republic of China, Standardization Administration of the People's Republic of China. Proximate Analysis of Solid Biofuels. Standard Publishing Press: Beijing, China, 2012.
30. Soria-Verdugo, A.; Guil-Pedrosa, J.F.; García-Hernando, N.; Ghoniem, A.F. Evolution of solid residue composition during inert and oxidative biomass torrefaction. *Energy* **2024**, *312*, 133486. https://doi.org/10.1016/j.energy.2024.133486.
31. *GB/T 21354-2008[S]*; General Administration of Quality Supervision, Inspection and Quarantine of the People's Republic of China, Standardization Administration of the People's Republic of China. Powders—Determination of Tap Density. Standard Publishing Press: Beijing, China, 2008.
32. Lam, P.S.; Sokhansanj, S.; Bi, X.; Lim, C.J.; Melin, S. Energy Input and Quality of Pellets Made from Steam-Exploded Douglas Fir (*Pseudotsuga menziesii*). *Energy Fuels* **2011**, *25*, 1521–1528. https://doi.org/10.1021/ef101683s.

33. Xia, X.; Sun, Y.; Wu, K.; Jiang, Q. Optimization of a straw ring-die briquetting process combined analytic hierarchy process and grey correlation analysis method. *Fuel Process. Technol.* **2016**, *152*, 303–309. https://doi.org/10.1016/j.fuproc.2016.06.018.
34. Liu, Z.; Liu, X.; Fei, B.; Jiang, Z.; Cai, Z.; Yu, Y. The properties of pellets from mixing bamboo and rice straw. *Renew. Energy* **2013**, *55*, 1–5. https://doi.org/10.1016/j.renene.2012.12.014.
35. Kaewtrakulchai, N.; Wongrerkdee, S.; Chalermsinsuwan, B.; Samsalee, N.; Huang, C.-W.; Manatura, K. Hydrophobicity and performance analysis of beverage and agricultural waste torrefaction for high-grade bio-circular solid fuel. *Carbon Resources Conversion* **2024**, 48, 100243. https://doi.org/10.1016/j.crcon.2024.100243.
36. Si, Y.; Hu, J.; Wang, X.; Yang, H.; Chen, Y.; Shao, J.; Chen, H. Effect of Carboxymethyl Cellulose Binder on the Quality of Biomass Pellets. *Energy Fuels* **2016**, *30*, 5799–5808. https://doi.org/10.1021/acs.energyfuels.6b00869.
37. Eisenbies, M.H.; Volk, T.A.; Therasme, O.; Hallen, K. Three bulk density measurement methods provide different results for commercial scale harvests of willow biomass chips. *Biomass Bioenergy* **2019**, *124*, 64–73. https://doi.org/10.1016/j.biombioe.2019.03.015.
38. Kellogg, R.M.; Wangaard, F.F. Variation in the cell-wall density of wood. *Wood Fiber Sci.* **2007**, *1*, 180–204. Available online: https://wfs.swst.org/index.php/wfs/article/view/1352 (accessed on 11 November 2024).
39. Quyen, V.T.; Nagy, S.; Faitli, J.; Csoke, B. Determination of radial pressure distribution on the wall of the press channel of a novel biomass single die pelletiser. *Eur. J. Wood Wood Prod.* **2020**, *78*, 1075–1086. https://doi.org/10.1007/s00107-020-01585-y.
40. Dai, X.; Theppitak, S.; Yoshikawa, K. Pelletization of Carbonized Wood Using Organic Binders with Biomass Gasification Residue as an Additive. *Energy Fuels* **2019**, *33*, 323–329. https://doi.org/10.1021/acs.energyfuels.8b03372.
41. Granado, M.P.P.; Suhogusoff, Y.V.M.; Santos, L.R.O.; Yamaji, F.M.; De Conti, A.C. Effects of pressure densification on strength and properties of cassava waste briquettes. *Renew. Energy* **2021**, *167*, 306–312. https://doi.org/10.1016/j.renene.2020.11.087.
42. Kashaninejad, M.; Tabil, L.G. Effect of microwave–chemical pre-treatment on compression characteristics of biomass grinds. *Biosyst. Eng.* **2011**, *108*, 36–45. https://doi.org/10.1016/j.biosystemseng.2010.10.008.
43. Rezaei, H.; Lim, C.J.; Lau, A.; Sokhansanj, S. Size, shape and flow characterization of ground wood chip and ground wood pellet particles. *Powder Technol.* **2016**, *301*, 737–746. https://doi.org/10.1016/j.powtec.2016.07.016.
44. De-Yu, T.U.; An-Xin, L.I.; Yun, H.U.; Wei, X. Lab-scale Experimental Study on the Compressing Molding Parameters Under Cold Condition for Rice Straw Pellets. *Chin. J. Agrometeorol.* **2015**, *36*, 446–453. https://doi.org/10.3969/j.issn.1000-6362.2015.04.008.
45. Pradhan, P.; Mahajani, S.M.; Arora, A. Production and utilization of fuel pellets from biomass: A review. *Fuel Process. Technol.* **2018**, *181*, 215–232. https://doi.org/10.1016/j.fuproc.2018.09.021.
46. He, H.; Wang, Y.; Sun, W.; Sun, Y.; Wu, K. Effects of different biomass feedstocks on the pelleting process and pellet qualities. *Sustain. Energy Technol. Assess.* **2024**, *69*, 103912. https://doi.org/10.1016/j.seta.2024.103912.
47. Nielsen, S.K.; Mandø, M.; Rosenørn, A.B. Review of die design and process parameters in the biomass pelleting process. *Powder Technol.* **2020**, *364*, 971–985. https://doi.org/10.1016/j.powtec.2019.10.051.
48. Liu, Z.; Zhang, F.-S. Effects of various solvents on the liquefaction of biomass to produce fuels and chemical feedstocks. *Energy Convers. Manag.* **2008**, *49*, 3498–3504. https://doi.org/10.1016/j.enconman.2008.08.009.
49. Simons, S.J.R. Chapter 27 Liquid bridges in granules. In Handbook of Powder Technology, Salman, A.D.; Hounslow, M.J.; Seville, J.P.K., Eds. Elsevier Science B.V.: 2007; Vol. 11, pp 1257-1316. https://doi.org/10.1016/S0167-3785(07)80062-5.
50. Lekounougou, S.; Kocaefe, D. Comparative study on the durability of heat-treated White Birch (*Betula papyrifera*) subjected to the attack of brown and white rot fungi. *Wood Mater. Sci. Eng.* **2012**, *7*, 101–106. Available online: https://api.semanticscholar.org/CorpusID:84460178 (accessed on 30 December 2024 ).
51. Liu, Z.; Zhang, F.-S. Removal of copper (II) and phenol from aqueous solution using porous carbons derived from hydrothermal chars. *Desalination* **2011**, *267*, 101–106. https://doi.org/10.1016/j.desal.2010.09.013.